Available online at www.sciencedirect.com
SCIENCE DIRECT®
Journal of Invertebrate Pathology 84 (2003) 198–213
Journal of INVERTEBRATE PATHOLOGY
www.elsevier.com/locate/yjipa

Ultrastructural characteristics and small subunit ribosomal DNA sequence of *Vairimorpha cheracis* sp. nov., (Microspora: Burenellidae), a parasite of the Australian yabby, *Cherax destructor* (Decapoda: Parastacidae)

Elizabeth G. Moodie,[a,*] Leo F. Le Jambre,[b] and Margaret E. Katz[c]

[a] *Department of Zoology, School of Biological, Biomedical and Molecular Sciences, University of New England, Armidale, NSW 2351, Australia*
[b] *CSIRO Livestock Industries, Locked Bag 1, Armidale, NSW 2350, Australia*
[c] *Department of Molecular and Cellular Biology, School of Biological, Biomedical and Molecular Sciences, University of New England, Armidale, NSW 2351, Australia*

Received 16 June 2003; accepted 10 November 2003

Abstract

This is the first record of a species of *Vairimorpha* infecting a crustacean host. *Vairimorpha cheracis* sp. nov. was found in a highland population of the Australian freshwater crayfish, *Cherax destructor*. The majority of spores and earlier developmental stages of *V. cheracis* sp. nov. were found within striated muscle cells of the thorax, abdomen, and appendages of the crayfish. Only octosporoblastic sporogony within sporophorous vesicles (SPVs) was observed. Diplokaryotic sporonts separated into two uninucleate daughter cells, each of which gave rise to four sporoblasts in a rosette-shaped plasmodium, so that eight uninucleate spores were produced within the persistent ovoid SPV. Ultrastructural features of stages in the octosporoblastic sequence were similar to those described for *Vairimorpha necatrix*, the type species. Mature spores were pyriform in shape and averaged $3.4 \times 1.9\,\mu m$ in dimensions. The anterior polaroplast was lamellar in structure, and the posterior polaroplast vesicular. The polar filament was coiled 10–12 times, lateral to the posterior vacuole. The small subunit ribosomal DNA (SSU rDNA) of *V. cheracis* sp. nov. was sequenced and compared with other microsporidia. *V. cheracis* sp. nov. showed over 97% sequence identity with *Vairimorpha imperfecta* and five species of *Nosema*, and only 86% sequence identity with *V. necatrix*. The need for a taxonomic revision of the *Nosema*/*Vairimorpha* group of species is discussed.

1. Introduction

The majority of microsporidia in the genera *Vairimorpha* Pilley and *Nosema* Naegeli are parasites of insects. *Vairimorpha* is found primarily in lepidopteran hosts, with the exception of *Vairimorpha invictae*, a parasite of the American fire ant *Solenopsis invicta* (Briano and Williams, 2002). *Nosema* is commonly found in Lepidoptera and Hymenoptera, although other taxa are parasitised, including Crustacea. For example, *Nosema granulosis* is a parasite of the marine amphipod *Gammarus duebeni* (Terry et al., 1999) and an undescribed species of *Nosema* was reported by Unestam (1973) to infect the British crayfish, *Austropotamobius pallipes*. Prior to this study, crustaceans have not been reported as hosts for *Vairimorpha* species.

The genus *Vairimorpha* was established by Pilley (1976) after *Thelohania diazoma* (Kramer, 1965), which has a octosporoblastic sequence resulting in uninucleate spores, was shown to be the same species as *Nosema necatrix*, which has the normal disporoblastic sequence typical of *Nosema* (Fowler and Reeves, 1974). The type description for *Nosema* does not include dimorphic developmental sequences or octosporoblastic sporogony. Consequently, *N. necatrix* was renamed *Vairimorpha necatrix* (Pilley, 1976). In the most recent taxonomic revision of the microsporidia by Sprague et al. (1992),

* Corresponding author. Fax: +61-2-677-338-14.
E-mail address: emoodie@pobox.une.edu.au (E.G. Moodie).

0022-2011/$ - see front matter © 2003 Elsevier Inc. All rights reserved.
doi:10.1016/j.jip.2003.11.004

Vairimorpha was placed in the Family Burenellidae (Jouvenaz and Hazard, 1978), and *Nosema* in the Family Nosematidae (Labbe, 1899).

The descriptions for the type species *Vairimorpha necatrix* (Pilley, 1976) and *Nosema bombycis* (Naegeli, 1857) are based on morphological features of spores and earlier developmental stages (meronts and sporonts), characteristics of the parasite–host interface and the nature of sporogony sequences (Sprague et al., 1992). *V. necatrix* and *N. bombycis* infect lepidopteran hosts. *N. bombycis* is transmitted horizontally per os and transovarially, whereas *V. necatrix* is only transmitted horizontally.

Meronts and sporonts in both genera are binucleate with fused nuclei (diplokarya). Binucleate and uninucleate spores are produced by *V. necatrix*, whereas only binucleate spores are produced by *N. bombycis*. In both genera, binucleate spores are found in direct contact with host cell cytoplasm. Two types are produced: primary binucleate spores that develop early in infection and serve to transmit the parasite between tissues within a host; and secondary binucleate spores that develop later in infection and are spread between hosts by the oral route, after release of spores to the environment (Solter and Maddox, 1998). The uninucleate spores of *V. necatrix* are formed in groups of eight within an interfacial envelope (Sprague et al., 1992) also known as a sporophorous vesicle (SPV). The route of transmission for uninucleate spores in *Vairimorpha* species is unclear.

Molecular phylogenetic studies based on small subunit ribosomal DNA (SSU rDNA) data indicate that some *Vairimorpha* species are more closely related to *Nosema* species than to other *Vairimorpha* species and that separation of the two genera on the basis of the presence or absence of octospores may be artificial, calling into question the usefulness of the number and type of sporogony sequences as a distinguishing taxonomic feature (Baker et al., 1995). In molecular analyses, *V. necatrix*, *Nosema apis*, and several other *Nosema* species are consistently grouped together in one clade (Baker et al., 1995; Malone and McIvor, 1996; Muller et al., 2000; Terry et al., 1999) distinct from a sister clade containing *Vairimorpha imperfecta*, *N. bombycis*, *Nosema trichoplusiae*, and other *Nosema* species (Canning et al., 1999, 2002). Baker et al. (1997) hypothesised that species with simple monomorphic life cycles may have secondarily lost one or more developmental sequences originally present in ancestors with more complex polymorphic life cycles.

In addition to the undescribed species of *Nosema* noted by Unestam (1973), microsporidian genera recorded as parasites of freshwater crayfish include *Thelohania* (Lom et al., 2001; Moodie et al., 2003a,b; Sprague, 1950), *Vavraia* (Langdon, 1991), and *Pleistophora* (O'Donoghue et al., 1990; O'Donoghue and Adlard, 2000; Sprague, 1966). All species show marked muscle tissue tropism. Two new species; *Thelohania parastaci* and *Thelohania montirivulorum*, both parasites of the Australian yabby, *Cherax destructor*, have recently been described (Moodie et al., 2003a,b). *T. parastaci* was found in lowland populations of yabbies whereas *T. montirivulorum* was found in a highland population.

In this paper a third new, octosporoblastic microsporidian parasite of *C. destructor* is described. *Vairimorpha cheracis* sp. nov. was found in a highland, stream-dwelling population of the Australian yabby. The ultrastructure of spores and earlier life cycle stages, and the sequence of events leading to the formation of mature spores within octosporous vesicles are described. Phylogenetic relationships between *V. cheracis* sp. nov. and other *Vairimorpha* and *Nosema* species, based on SSU rDNA analyses, are presented. The reasons for placing this new species in the genus *Vairimorpha* are discussed.

2. Materials and methods

2.1. Source of specimens

Heavily infected yabbies of the subspecies *C. destructor destructor* (Austin, 1996), were caught using dipnets and traps in spring, summer and autumn, from Tea Tree Creek (30°30′S, 151°29′E) in the upper Gwydir River catchment 20 km west of Armidale, NSW, Australia. Tissue samples from two adult male yabbies and four adult female yabbies (Table 1) were preserved and processed as described below for light microscopy, electron microscopy, DNA extraction, PCR amplification, and sequencing of the SSU rDNA region.

2.2. Light microscopy

Microsporidian infection of yabbies was confirmed by examination of fresh squashes of anterior pleopod

Table 1
Microsporidian species infecting adult yabbies (*C. destructor*) from which samples were taken for microscopy and molecular studies

Date of capture	Sex of host	Microsporidian species present in the host	Sample code
3.5.99	M	*V. cheracis* sp. nov. & *T. montirivulorum*	T1
19.7.99	M	*V. cheracis* sp. nov.	T2
12.2.00	F	*V. cheracis* sp. nov & *T. montirivulorum*	T3
30.10.00	F	*V. cheracis* sp. nov. & *T. montirivulorum*	Tx1
10.12.00	F	*V. cheracis* sp. nov.	Tx2
28.2.01	F	*V. cheracis* sp. nov. & *T. montirivulorum*	Tx3

muscle at 1000× magnification under a Zeiss compound microscope. Impression smears of infected abdominal muscle were stained with 10% Giemsa (Undeen, 1997). Semi-thin sections of tissue processed for electron microscopy (see below) were stained with 1% toluidine blue. Samples of fresh abdominal muscle were stored frozen and later thawed for spores to be photographed and measured. Measurements were made using Photoshop 5.5 (Adobe, San Jose, USA) software.

2.3. Electron microscopy

Samples of fresh abdominal muscle, hepatopancreas, intestine, and ovary were fixed overnight at 4 °C in a mixture of 2% gluteraldehyde, 2% paraformaldehyde, and 0.5% dimethyl sulfoxide in 0.1 M cacodylate buffer containing 8 mM $CaCl_2$ (J. Mathews, pers. com.). Fixed tissues were washed five times in fresh 0.1 M cacodylate buffer and postfixed for 1–2 h in 1% osmium tetroxide. A 2% uranyl acetate bloc stain was performed at the second stage of dehydration through a graded acetone series. Tissue blocks were embedded in Spurr's resin. Ultrathin sections were post stained in 4% uranyl acetate (w/v) and 0.25% lead citrate (w/v) prior to examination with a Jeol JEM 1200 EX electron microscope, operated at 60 kV.

2.4. DNA extraction

Spores from approximately 0.5 g of heavily infected abdominal muscle were purified by digestion in 10 ml 2% pepsin (w/v) in 0.5% HCl (v/v) for 1 h at 37 °C (Langdon, 1991), pelleted by centrifugation at 1800*g* for 10 min and washed in sterile distilled water four times. The spore pellet was suspended in 50 µl of extraction buffer (100 mM NaCl, 10 mM Tris–HCl, pH 8.0, 25 mM EDTA, and 0.5% SDS), frozen and thawed three times, and then ground for 30 s in a 1.5 ml microfuge tube with a micropestle attached to a a hand held electric drill. Four hundred and fifty milliliters of extraction buffer was added and the suspension incubated overnight at 37 °C with proteinase K (200 µg per ml). The proteinase K was inactivated by heating the solution for 5 min at 95 °C. After cooling to room temperature, the extract was incubated with RNase (100 µg per ml) for 30 min at 37 °C.

Genomic DNA in the digestion solution was purified by extraction in phenol/chloroform/isoamyl alcohol (25:24:1), followed by extraction in chloroform/isoamyl alcohol (24:1). The purified DNA was precipitated with ethanol, dissolved in 100 µl of TE buffer (10 mM Tris–HCl, pH 8.0, 1 mM EDTA) at 65 °C for 1 h, and stored at −20 °C. DNA concentration and purity were determined spectrophotometrically by measuring absorbance at wavelengths of 260 and 280 nm.

2.5. PCR amplification of SSU rDNA

The universal primers 18f and 1492r (Weiss and Vossbrinck, 1998) were used to amplify the SSU rDNA (Table 2). Each 50 µl PCR mix contained 5 µl of 10× reaction buffer without $MgCl_2$ (Promega, Madison, USA), 1.5 mM $MgCl_2$, 0.2 mM dNTPs, 25 pmol of each primer, 1.25 U of *Taq* DNA polymerase (Promega, Madison, USA) and 120 ng of template DNA. PCR amplifications were performed as follows on a Mastercycler Gradient thermocycler (Eppendorf, Hamburg, Germany): after an initial denaturation for 2 min at 94 °C, samples were subjected to 35 cycles of amplification (denaturation at 94 °C for 1 min, primer annealing at 48 °C for 1 min, and extension at 68 °C for 2 min), followed by a 10 min final extension at 68 °C. A DNA fragment of 1203 bp in length (including primers) was amplified, purified with the Wizard PCR Preps Purification System (Promega, Madison, USA) and sequenced directly, as described below.

2.6. Sequencing

Sequencing was performed by Newcastle DNA (University of Newcastle, NSW, Australia) using Big Dye Kit dye terminator chemistry and an automated ABI PRISM 377 DNA Sequencer (Applied Biosystems, Richmond, USA). The universal primers 18f and 1492r and internal primers V306f, T423f, T423r, and V420r were used for sequencing (Table 2).

2.7. Phylogenetic analyses

SSU rDNA sequences from 24 microsporidians, including *V. cheracis* sp. nov. (Table 3), were aligned with Clustal X version 1.81 (Jeanmougin et al., 1998). The microsporidian *Antonospora scoticae* was chosen as the outgroup because of its basal position relative to all other species in trees produced by phylogenetic analyses of a wide range of species from the phylum Microspora (Lom et al., 2001; Moodie et al., 2003b) Phylogenetic analyses were performed with PAUP* version 4.0b9 for

Table 2
Sequencing primers for SSU rDNA of *V. cheracis* sp. nov.

Primer	5′ → 3′ sequence	Melting temperature (°C)
Forward		
18f	CACCAGGTTGATTCTGCC	56.0
V306f	GGCGAAACTTGACCTATGAT	60.5
T423f	GGCTTAATTTGACTCAACGC	58.0
Reverse		
1492r	GGTTACCTTGTTACGACTT	54.0
T423r	GCGTTGAGTCAAATTAAGCC	55.3
V420r	AACAAGTATTACCGCGGCTG	60.0

Table 3
Hosts and GenBank Accession numbers for SSU rDNA of 24 microsporidia used in phylogenetic analyses

Organism	Host (I, insect; C, crustacean)	GenBank Accession No.
Antonospora scoticae	*Andrena scotica* (I)	AF024655
Microsporidium sp.	*Talorchestia deshayesei* (C)	AJ438963
Nosema apis	*Apis mellifera* (I)	X73894
Nosema bombycis	*Bombyx mori* (I)	D85504
Nosema ceranae	*Apis cerana* (I)	U26533
Nosema furnacalis	*Ostrinia furnacalis* (I)	U26532
Nosema granulosis	*Gammarus duebeni* (C)	AJ011833
Nosema oulemae	*Oulema melanopus* (I)	U27359
Nosema sp. NIS M11	*Bombyx mori* (I)	D85501
Nosema trichoplusiae	*Apis cerana* (I)	U09282
Nosema tyriae	*Tyria jacobaeae* (I)	AJ012606
Nosema vespula[a]	*Vespula germanica* (I)	U11047
Thelohania contejeani C2	*Astacus fluviatilis* (C)	AF492593
Thelohania montirivulorum	*Cherax destructor* (C)	AY183664
Thelohania parastaci	*Cherax destructor* (C)	AF294780
Thelohania solenopsae	*Solenopsis invicta* (I)	AF031538
Thelohania sp. FA	*Solenopsis richteri* (I)	AF031537
Vairimorpha imperfecta	*Plutella xylostella* (I)	AJ131645
Vairimorpha necatrix	*Pseudaletia unipuncta* (I)	Y00266
Vairimorpha cheracis sp. nov.	*Cherax destructor* (C)	AF327408
Vairimorpha sp. FA	*Solenopsis richteri* (I)	AF031539
Vairimorpha sp. GER	*Plutella xylostella* (I)	AF124331
Vairimorpha sp. NIS M12	*Bombyx mori* (I)	D85502
Visvesvaria algerae[b]	mosquito (I)	AF024656

[a] Although lodged in GenBank as *Nosema vespula*, it is not a legitimate species name.
[b] *Visvesvaria algerae* is now considered to be *Brachiola algerae* (Cali et al., 1998).

Windows (Swofford, 2000), and MrBayes (Huelsenbeck and Ronquist, 2001), on an IBM compatible personal computer (PC). Trees were constructed by PAUP using neighbour-joining distance criteria, maximum parsimony criteria (branch and bound method), maximum likelihood criteria and by Bayesian inference (MrBayes). The general time reversible (GTR) model, which allows for unequal nucleotide frequencies and six substitution types (Swofford, 2000), was used for tree construction. The optimum evolutionary model for maximum likelihood or Bayesian analyses was determined using the program ModelTest 3.06 (Posada and Crandall, 1998) with ancillary software, provided by Dr. F.P. Patti (pers. com.), to facilitate analysis on a PC. Bootstrap values for the distance and parsimony trees were calculated with 10,000 repetitions in each analysis. When Bayesian analyses were performed, base frequencies, proportion of sites differing, transition to transversion ratios and the γ-shape parameter were calculated from the data. 1,000,000 iterations were carried out for the MrBayes analysis, with 100 iterations per tree saved.

3. Results

Spores of *V. cheracis* sp. nov. were found at very high densities in striated muscle cells in the thorax, abdomen, and appendages of yabbies, often in mixed infections with *T. montirivulorum* (Moodie et al., 2003b). Where mixed infections occurred, *V. cheracis* sp. nov. could be differentiated from *T. montirivulorum* on the basis of spore shape, size, and ultrastructural characteristics, SPV ultrastructure, and by differences in SSU rDNA sequence, as described below. In all crayfish examined, the majority of spores of *V. cheracis* sp. nov. occurred in groups of eight within persistent sporophorous vesicles (SPVs). Binucleate sporonts could be identified as belonging to *V. cheracis* sp. nov. rather than *T. montirivulorum* on the basis of ultrastructural features, where mixed infections were present in the same host tissues. Few meronts were present in the tissues of the yabbies examined.

The abdominal muscle of heavily infected individuals appeared white and opaque when viewed through the carapace. These animals did not feed, moved abnormally slowly, and usually died if moulting occurred. No heavily infected juvenile crayfish were found. Yabbies with grossly visible signs of infection were maintained in aquaria for up to six months prior to death, suggesting a slow rate of progress of infection. Overall prevalence of infection by *V. cheracis* sp. nov., determined by microscopic examination of pleopod tissue from 645 yabbies caught between January 2000 and February 2002, was 5.0%. Prevalence of infection in yabbies from different regions of Tea Tree Creek varied from 3.0% to 12.2% over the same period. Hapantotype (sample Tx2, Table 1) and parahapantotype (sample Tx1, Table 1)

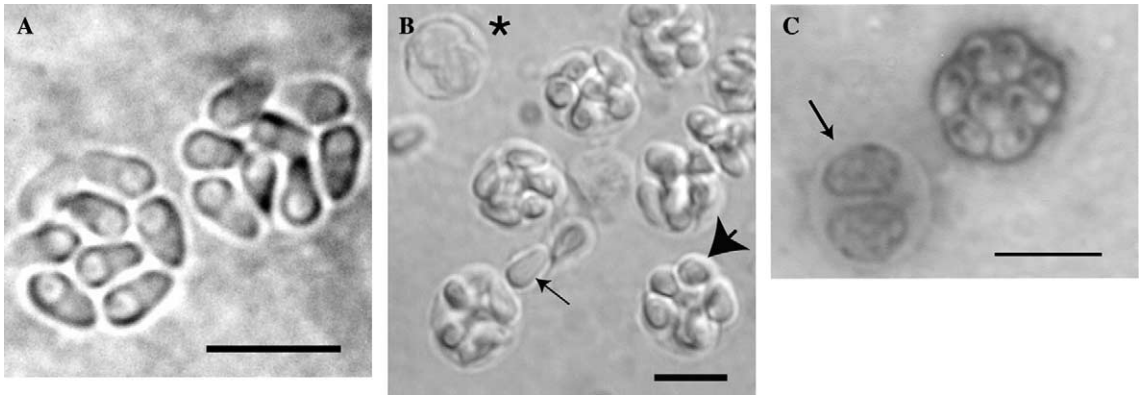

Fig. 1. Light micrographs of *V. cheracis* sp. nov. (A) Two fresh sporophorous vesicles (SPVs), each with eight pyriform spores, (B) fresh octosporous SPVs (large arrow), single spores released from ruptured SPVs (small arrow), and two sporont daughter cells within an SPV (*), (C) Giemsa-stained smear of an octosporous SPV and an SPV containing a sporont with separated nuclei (arrow). Scale bars 5 μm.

specimens of *V. cheracis* sp. nov. were lodged with the Queensland Museum, Brisbane, Australia (Registration numbers G463720 and G463721, respectively).

3.1. Light microscopy

Spores of *V. cheracis* sp. nov. were markedly pyriform in shape, with the posterior vacuole located at the wider end (Fig. 1A). After storage at −20 °C, spores in freshly thawed muscle tissue averaged 3.4 (3.0–3.8) μm in length and 1.9 (1.7–2.3) μm in width ($n = 40$). SPVs were spherical in shape (Fig. 1B) and when thawed, averaged 6.6 (5.9–7.4) μm in diameter ($n = 40$). Spores were packed tightly in robust SPVs, so that few spores were released when pressure was applied to the coverslip during the preparation of muscle squashes. Single spores released from ruptured SPVs can be seen in Fig. 1B. Eight uninucleate spores within an SPV are clearly visible in Fig. 1C. A sporont in which nuclear separation has occurred is visible adjacent to the SPV in the same figure. The photographs were taken of squash and smear preparations from a yabby (Tx2) that was infected only by *V. cheracis* sp. nov.

3.2. Electron microscopy

Meronts were rare, presumably because the yabbies sampled were at an advanced stage of infection. They were only seen in yabbies co-infected with *V. cheracis* sp. nov. and T. *montirivulorum* and it was not possible to unequivocally differentiate between the meronts of either species, therefore they were not included in this description. Differentiation of sporonts, SPVs, sporoblasts and uninucleate spores of *V. cheracis* sp. nov. from those of *T. montirivulorum* was possible because these stages were found in yabbies infected with only one or the other microsporidian species, as well as in co-infected yabbies.

3.3. Sporonts, sporoblasts, and SPVs

Sporont development in *V. cheracis* sp. nov. was similar to the pattern described for *V. necatrix* (Mitchell and Cali, 1993). Sporonts of *V. cheracis* sp. nov. were binucleate with the nuclei initially closely apposed to form a diplokaryon (Fig. 2), prior to separation during sporogenesis. It could not be determined whether the two nuclei simply moved apart or whether they fused and then divided prior to partial cytokinesis. Endoplasmic reticulum was prominent in early sporonts (Figs. 2 and 3), but not in later sporonts, in which strands of granular cytoplasm extended around numerous vesicles (Figs. 4 and 5).

Fig. 2. Early diplokaryotic sporont showing closely apposed nuclei (n) and coils of endoplasmic reticulum. Scale bar 200 nm.

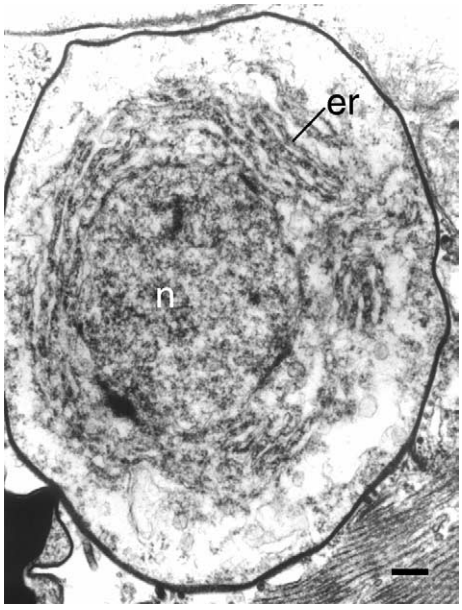

Fig. 3. Early sporont with only one nucleus (n) visible in the section plane. Ribbons of endoplasmic reticulum (er) appear more condensed than in Fig. 2. Scale bar 200 nm

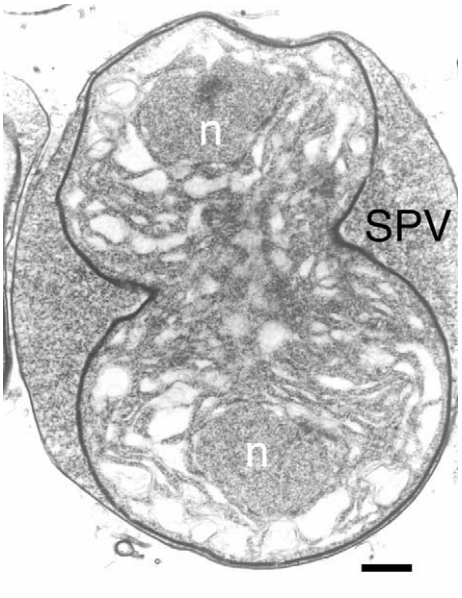

Fig. 5. A sporont in the process of dividing inside a sporophorous vesicle (SPV). A prominent nucleolus is visible in the upper nucleus (n). Scale bar 500 nm.

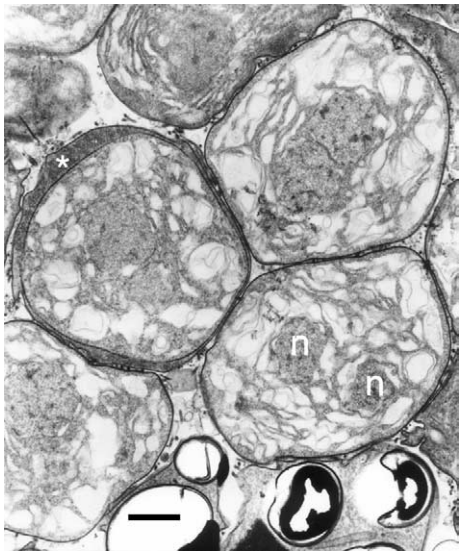

Fig. 4. Binucleate sporonts. The nuclei (n) in the sporont on the lower right appear to have dissociated. A SPV (*) has formed around the sporont on the left. Scale bar 1 μm.

Formation of SPVs around sporonts was initiated prior to cytokinesis of sporont daughter cells and fragments of electron dense material, reminiscent of chromosomes, could be seen in the nuclei of sporonts at this time (Fig. 4). A well-developed SPV containing granular material in the episporontal space can be seen surrounding the dumbbell-shaped sporont in Fig. 5. Migration of the nuclei to opposite poles of the dumbbell preceded division of the sporont daughter cells. Further nuclear division followed so that a rosette-shaped plasmodium was formed. It was unclear whether the two daughter sporont cells completely separated to form four sporoblasts each or remained attached at the centre to form an octolobate plasmodium from which eight sporoblasts were pinched off. No more than four contiguous lobes were seen in any sections of sporogonial plasmodiums. This pattern is very similar to the octosporous sporogony sequence described for *V. necatrix* by Mitchell and Cali (1993).

The episporontal space of sporophorous vesicles of *V. cheracis* sp. nov. was filled with fine granular cytoplasm (Figs. 5–7). Electron dense granular material, tubular inclusions 70–80 nm in diameter, and occasionally larger dense inclusions, were evident in some sections. They appeared to be associated with development of the sporoblast walls, prior to separation of the plasmodium into discreet sporoblasts (Fig. 6).

Within each SPV, eight uninucleate sporoblasts, each surrounded by an electron dense layer of fairly even thickness, were pinched off from the rosette-shaped plasmodium (Fig. 7). Masses of endoplasmic reticulum were apparent in sporoblasts at the time that spore organelle formation was initiated (Fig. 8). The polar filament was the first new organelle to form within sporoblasts, followed by the anchoring disc and the polar capsule (Fig. 9) and finally the posterior vacuole (Fig. 10). The number of coils of the polar filament increased as sporoblasts matured, and the exospore layer thickened. In mature spores, the polar filament was coiled up to 12 times. Sporoblasts changed in shape from oval to pyriform during the maturation process.

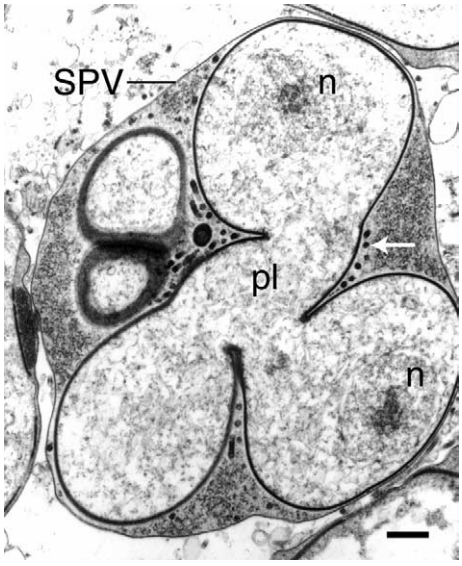

Fig. 6. Rosette-shaped plasmodium (pl), showing two nuclei (n) with prominent nucleoli in two of the lobes. Tubular inclusions (arrow) in the cytoplasm of the SPV are evident close to the plasmodium wall. Scale bar 500 nm.

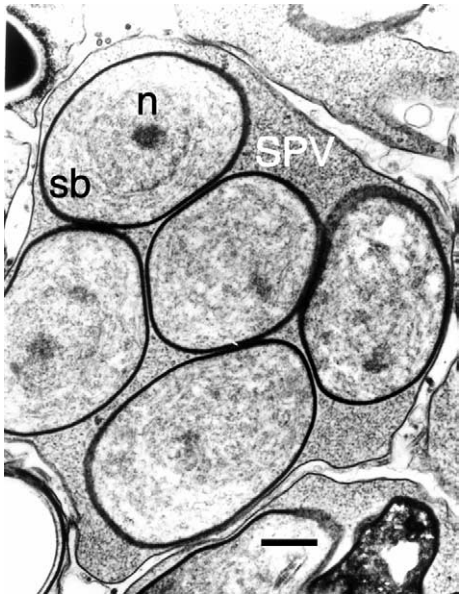

Fig. 7. Sporophorous vesicle (SPV) with five of eight sporoblasts visible in the section. Each sporoblast (sb) has a single nucleus (n). Scale bar 500 nm.

The characteristic pyriform shape of *V. cheracis* sp. nov. spores is evident in the sporoblast in Fig. 10. Electron dense granules, similar in density and diameter to the core of the developing polar filament, were seen adjacent to the posterior vacuole in late sporoblasts (Fig. 11). The granules may be involved in the formation of the distal end of the polar filament.

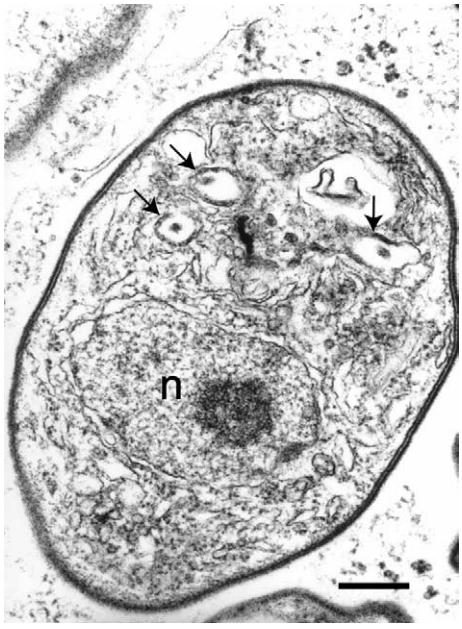

Fig. 8. Sporoblast with a well-defined single nucleus (n) and large nucleolus. The first coils of the polar filament (arrows) are evident. Scale bar 200 nm.

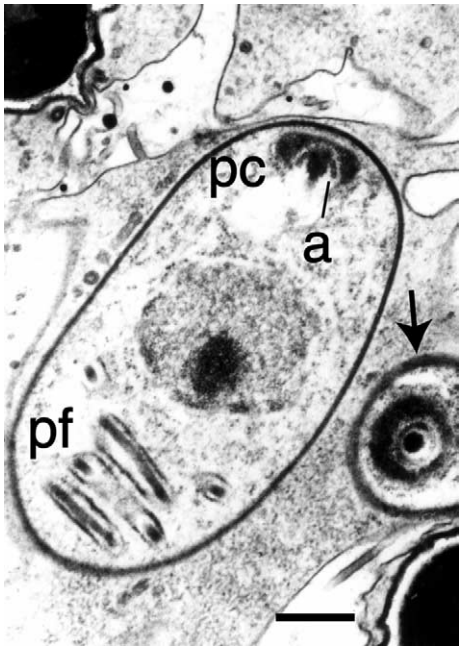

Fig. 9. Sporoblast with a crescent-shaped polar capsule (pc) cupped around the anchoring disc (a). The polar filament (pf) is coiled four times in the posterior region of the cell. To the right is a spore sectioned transversely through the polar capsule region (arrow). Scale bar 500 nm.

3.4. Mature spores

Only uninucleate spores of *V. cheracis* sp. nov. were found during this study. Features which allowed differentiation of *V. cheracis* sp. nov. and *T. montirivulorum*,

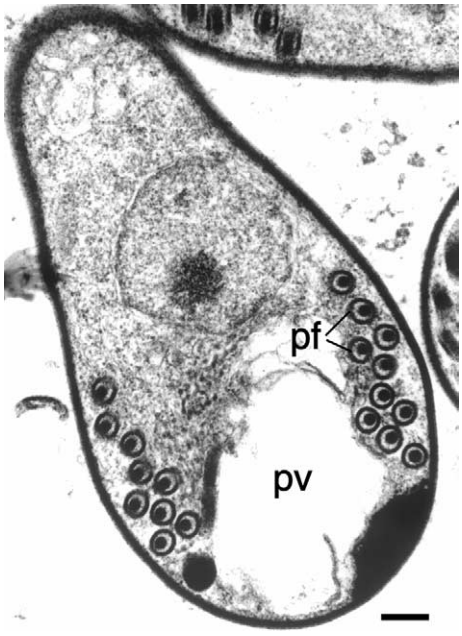

Fig. 10. Late sporoblast with 10 coils of the polar filament (pf) adjacent to the posterior vacuole (pv). Scale bar 200 nm.

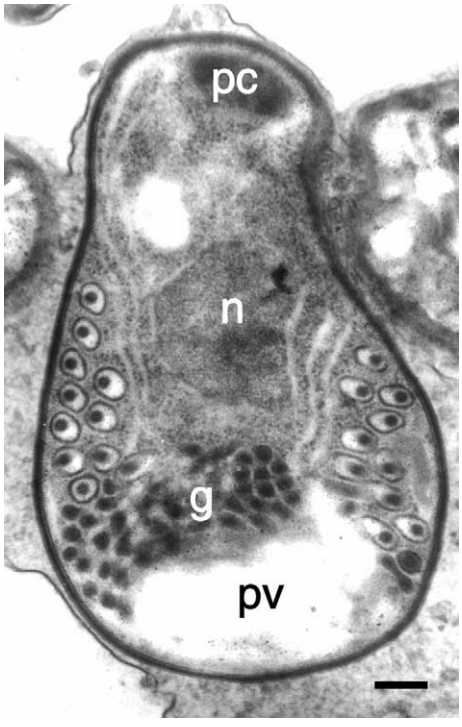

Fig. 11. Mature sporoblast showing the polar capsule region (pc), a single nucleus (n) and numerous electron dense granules (g) between the last coils of the polar filament and the posterior vacuole (pv). Scale bar 200 nm.

where the same host tissues were co-infected, are described in Table 4. The endospore layer was formed at a late stage of spore maturation (Fig. 12). The average thicknesses of the electron dense exospore and electron lucent endospore layers of *V. cheracis* sp. nov. were 31 nm and 52 nm ($n = 10$), respectively. No filamentous projections from the exospore layer were observed.

The electron dense anterior polaroplast was composed of tightly packed parallel membranes (Fig. 13) whereas the posterior polaroplast was more vesicular in nature and did not take up as much stain (Fig. 14). The isofilar polar filament descended in a straight line from the anchoring disc of the polar capsule, through the polaroplast, to the posterior pole of the nucleus where it coiled 10–12 times, lateral to both nucleus and posterior vacuole (Fig. 12). The average diameter of the polar filament was 82 nm ($n = 50$). Ultrastructural features shared by the uninucleate spores of *V. cheracis* sp. nov. and *V. necatrix* (Table 4) include the isofilar nature of the polar filament, a lamellar anterior polaroplast and more vesicular posterior polaroplast, and a polar capsule with an outer layer which extends for approximately three times the length of the outer layers of the anchoring disk (Fig. 13). The polar filament was coiled 13–14 times in most uninucleate spores of *V. necatrix*, whereas a slightly lower number of coils (10–12) were found in *V. cheracis* sp. nov. The spores of *V . cheracis* sp. nov. were pyriform in shape rather than oval as described for *V. necatrix* (Mitchell and Cali, 1993).

Although most spores were found within muscle cells in the abdomen, thorax, and appendages of yabbies, small numbers were also observed within the mucosa of the anterior intestine (Fig. 15), and in ovarian tissue (Fig. 16). The spores in the intestinal mucosa were within a SPV inside an interstitial cell sandwiched between muscle and epithelial cells. Those in the ovary were in SPVs in an intercellular space between follicular cells surrounding the ovum. Spores were not found within haemocytes or in haemolymph, however yabbies with recently acquired infections were not examined.

3.5. SSU rDNA sequence

The SSU rDNA sequence of *V. cheracis* sp. nov. from sample T1 (Table 1) was submitted to GenBank (Accession No. AF327408). This sequence was identical to the SSU rDNA sequences obtained from samples Tx1 and Tx2. Including the primers 18f and 1492r, the rDNA was 1203 bp in length. When SSU rDNA sequences were compared, *V. cheracis* sp. nov. showed over 97% sequence identity with the insect pathogens *Nosema furnacalis*, *N. trichoplusiae*, *N. bombycis*, *Nosema tyriae*, *V. imperfecta*, and *Vairimorpha* sp. GER., and the amphipod parasite *N. granulosis* (Table 5). Eighty-six percentage sequence identity was shared between *V. cheracis* sp. nov. and the type species *V. necatrix*. Higher levels of sequence identity were shown between *V. cheracis* sp. nov. and the yabby parasites *T. parastaci* and *T. montirivulorum* (73.2% and 72.8%,

Table 4
Comparison of morphological and ultrastructural features of *T. montirivulorum*, *V. cheracis* sp. nov., and *V. necatrix*

Feature	*T. montirivulorum* (Moodie et al., 2003ab)	*V. cheracis* sp. nov.	*V. necatrix* (Pilley, 1976; Mitchell and Cali, 1993)
Host	Decapoda: Parastacidae *Cherax destructor* (Clark)	Decapoda: Parastacidae *Cherax destructor* (Clark)	Lepidoptera: Noctuidae *Pseudaletia unipunctata* (Haworth)
Spore shape	Elongate, cylindrical, rounded ends	Pyriform, narrower anterior end	Uninucleate: ovoid Binucleate: elongate, cylindrical
Free binucleate spore length (μm)	5.9 (4.9–7.2) thawed, unstained	Binucleate spores not found	4.3 (3.9–5.0) Giemsa-stained
Free binucleate spore width (μm)	2.6 (2.0–3.1) thawed, unstained	Binucleate spores not found	2.3 (2.0–2.7) Giemsa-stained
Uninucleate octospore length (μm)	>3.4, thawed, unstained. More accurate measurement not possible	3.4 (3.0–3.8) unstained	1.9 (1.5–2.0) Giemsa-stained
Uninucleate octospore width (μm)	>2.0, thawed, unstained. More accurate measurement not possible	1.9 (1.7–2.3) unstained	1.1 (1.0–1.3) Giemsa stained
Polaroplast (anterior/posterior)	Lamellar/lamellar	Lamellar/vesicular	Lamellar/vesicular
No. coils in polar filament	20–22 in uninucleate and binucleate spores	10–12 in uninucleate spores	13–14 in uninucleate spores; 14–15 in binucleate spores
Polar filament diameter	Isofilar	Isofilar	Isofilar
SPV diameter (μm)	8.4 (7.0–9.6)	6.6 (5.9–7.4)	6.37 (5.58–7.36)
Episporontal inclusions in SPVs	Macrotubules (130–250 nm in diameter) and microtubules (60–120 nm diameter) common	No macrotubules. Granular material and occasional tubular inclusions 70–80 nm in diameter	Tubular inclusions of variable diameter common, arranged in concentric layers in some sections
Diplokaryotic free spores present	Yes	Not observed	Yes
Octosporous vesicles with uninucleate spores	Yes	Yes	Yes

respectively) than between *V. cheracis* sp. nov. and the undescribed fire ant pathogen, *Vairimorpha* sp. FA (63.6%).

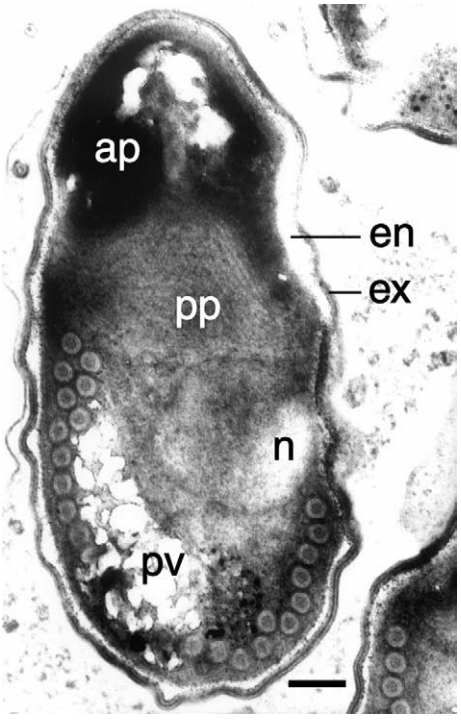

Fig. 12. Mature spore with darkly stained anterior polaroplast (ap), lightly stained posterior polaroplast (pp), relatively thick endospore layer (en) under the exospore layer (ex), single nucleus (n), and 11 coils of the polar filament adjacent to the posterior vacuole (pv). Scale bar 200 nm.

3.6. Phylogenetic analyses based on SSU rDNA sequences

On the basis of likelihood ratio tests and AIC criteria employed by the ModelTest program, the GTR model with rate heterogeneity (GTR + G + I) was indicated as

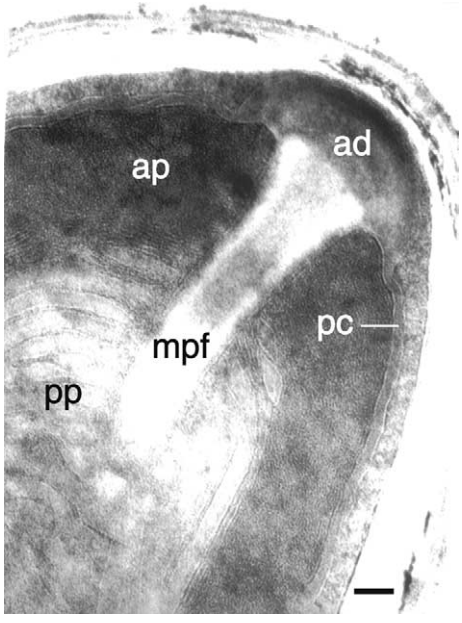

Fig. 13. Detail of anterior region of a mature spore showing the anchoring disc (ad), polar capsule (pc), anterior polaroplast (ap), posterior polaroplast (pp), and manubrium of the polar filament (mpf). Scale bar 50 nm.

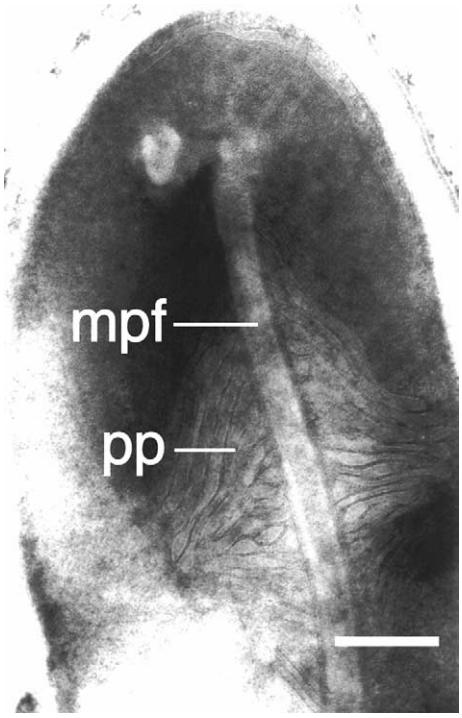

Fig. 14. Mature spore with vesicular posterior polaroplast (pp) bisected by manubrium of polar filament (mpf). Scale bar 200 nm.

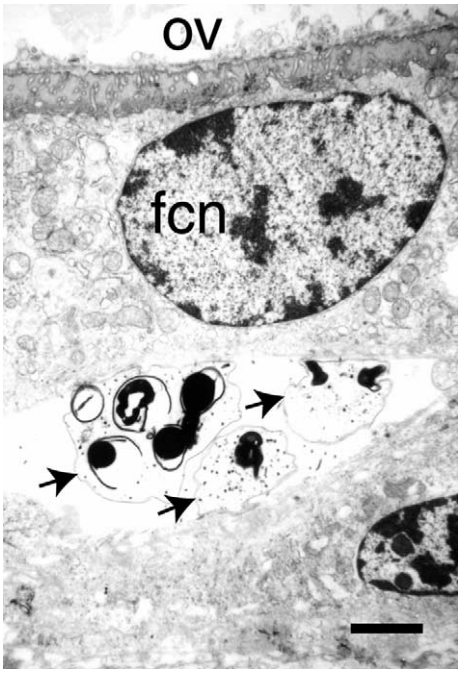

Fig. 16. Three SPVs (arrows) containing spore remnants, external to the layer of follicular cells which surround an ovum (ov). Each follicular cell has a large nucleus (fcn). Scale bar 2 μm.

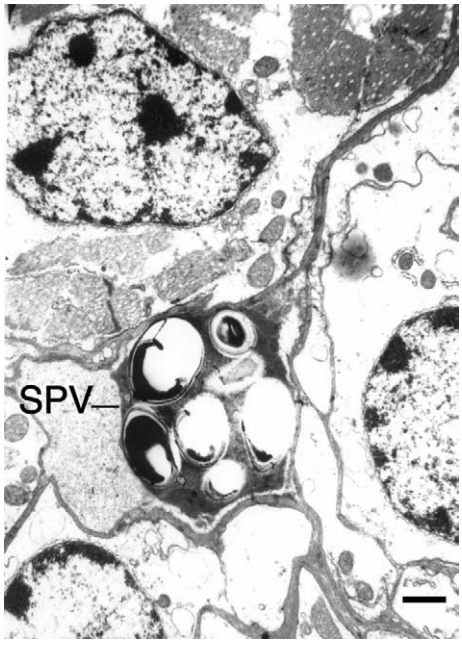

Fig. 15. Sporophorous vesicle (SPV) containing remnants of seven spores, sandwiched between three cells within the mucosa of the anterior intestine. Scale bar 1 μm.

the optimum model for Bayesian analyses of the data. The GTR + G + I model estimates from the data the gamma distribution for nucleotide substitution rates and the proportion of invariable sites. Tree lengths in the Bayesian analyses stabilised very quickly; the first 600 trees (6%) were discarded when calculating the frequencies of observed bipartitions.

Phylogenetic trees constructed using distance, parsimony, and Bayesian criteria were very similar in topology (Fig. 17). The branching patterns of the tree constructed using maximum likelihood criteria (not shown) were the same as in the tree constructed by Bayesian inference. The *Vairimorpha* and *Nosema* group of species, with the exception of the fire ant pathogen *Vairimorpha* sp. FA, were clustered together in a clade which was divided into two subclades. *V. cheracis* sp. nov. occupied a basal position in the subclade containing *V. imperfecta*, *Vairimorpha* sp. GER, *N. tyriae*, *N. trichoplusiae*, *N. bombycis*, *N. furnacalis*, and *N. granulosis.* This arrangement was supported by bootstrap values of 100% in the distance and parsimony trees and a bipartition frequency of 100% in the Bayesian tree. *V. cheracis* sp. nov. was invariably placed in a separate subclade to *V. necatrix*, *Vairimorpha* sp. M12, *N. apis*, *Nosema oulemae*, *Nosema* sp. M11, *Nosema vespula* and *N. ceranae* (Fig. 17).

The topology of trees based on distance and Bayesian analyses indicated that *V. cheracis* sp. nov. is probably most closely related to *N. granulosis* and *N. furnacalis*, however the relative positions of *V. cheracis* sp. nov., *N. granulosis* and *N. furnacalis* with respect to one another could not be resolved with the SSU rDNA data. The fire ant pathogen, *Vairimorpha* sp. FA was placed outside

Table 5
Sequence identities (SSU rDNA) between *V. cheracis* sp. nov. and other *Vairimorpha*, *Nosema* and *Thelohania* species

Organism	Host (I, insect; C, crustacean)	% Sequence identity with *V. cheracis* sp. nov.[a]
Nosema furnacalis	*Ostrinia furnacalis* (I)	97.9 (1130)
Nosema granulosis	*Gammarus duebeni* (C)	97.7 (1130)
Nosema trichoplusiae	*Apis cerana* (I)	97.6 (1131)
Nosema bombycis	*Bombyx mori* (I)	97.6 (1130)
Nosema tyriae	*Tyria jacobaeae* (I)	97.4 (1131)
Vairimorpha imperfecta	*Plutella xylostella* (I)	97.4 (1129)
Vairimorpha sp. GER	*Plutella xylostella* (I)	97.3 (1129)
Vairimorpha necatrix	*Pseudaletia unipuncta* (I)	86.0 (1165)
Nosema apis	*Apis mellifera* (I)	84.8 (1162)
Thelohania montirivulorum	*Cherax destructor* (C)	72.8 (1288)
Thelohania parastaci	*Cherax destructor* (C)	73.2 (1281)
Vairimorpha sp. FA	*Solenopsis richteri* (I)	63.6 (1275)

[a] Figure in brackets refers to number of nucleotides compared, with adjustment for gaps and ambiguities.

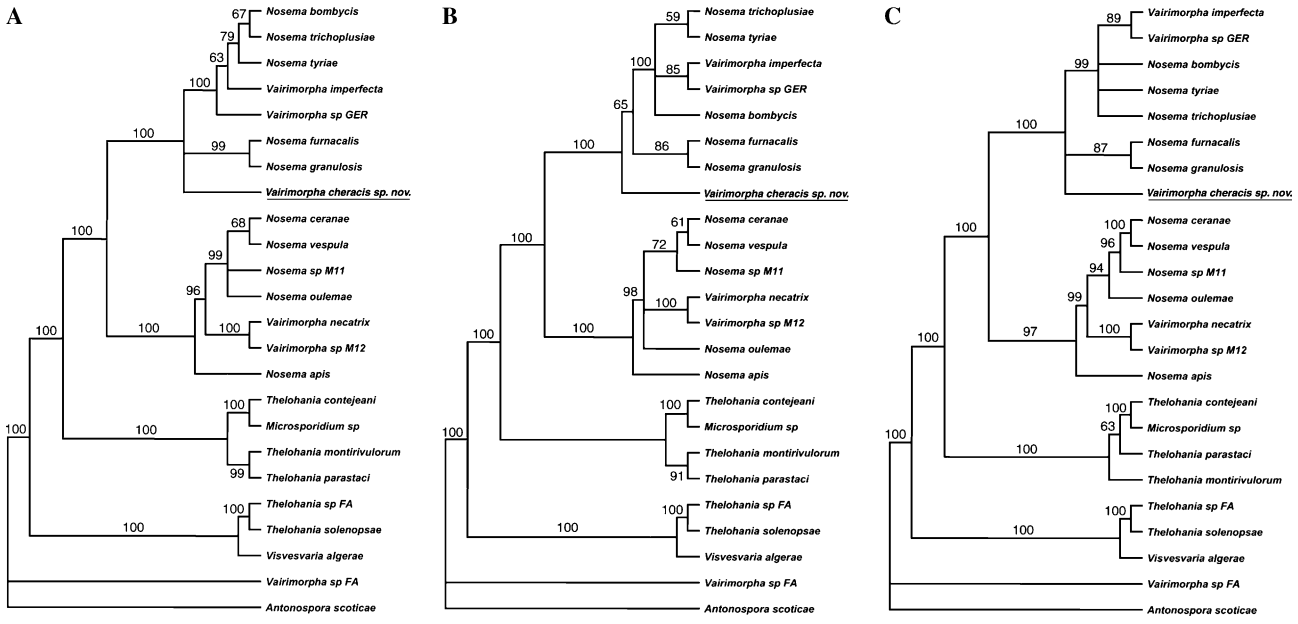

Fig. 17. Phylogenetic trees showing relationships between SSU rDNA from *Vairimorpha*, *Nosema*, *Thelohania*, and related species. Trees were constructed using distance criteria with the GTR model (A), maximum parsimony criteria (B) and Bayesian inference with the GTR + G + I model (C). Bootstrap values >50% are indicated on the branches of trees A and B. The frequencies of observed bipartitions are indicated on the branches of tree C. Values lower than 50% are not shown. *Antonospora scoticae* was used as the outgroup in all trees.

both the *Vairimorphal Nosema* clade and its sister clade, which included the freshwater crayfish parasites *T. parastaci*, *T. montirivulorum*, and *T. contejeani*.

Visvesvaria algerae, a member of the clade containing the fire ant parasites *Thelohania solenopsis* and *Thelohania* sp. FA, is more correctly described as *Brachiola algerae*. Although SSU rDNA sequence was lodged in GenBank as *Visvesvaria algerae*, the species was legitimately published as *Nosema algerae* by Vavra and Undeen (1970) (Muller et al., 2000). *N. algerae* was subsequently transferred to the genus *Brachiola* (Cali et al., 1998). Likewise, a more correct description for *N. vespula* is *Nosema* sp. from *Vespula* (a wasp). Although the sequence was lodged in GenBank as *N. vespula*, it is not a legitimate species name (Rice, 2001).

4. Discussion

Vairimorpha cheracis sp. nov. was placed in the genus *Vairimorpha* due to similarities with other members of the genus in ultrastructural characteristics of sporonts and octospores, developmental features associated with the octosporoblastic sequence and SSU rDNA sequence. The species name ''cheracis'' refers to the host, *Cherax destuctor*, in which the parasite was found. The type desciption for *V. necatrix* includes dimorphic development, with both disporoblastic sporogony and octosporoblastic sporogony occurring in the life cycle (Pilley, 1976). Only the latter form of sporogony was observed in yabbies heavily infected with *V. cheracis* sp. nov., however, in view of the advanced stage of infection

of the yabbies examined and the fact that many were co-infected with *T. montirivulorum* (a species that produces both binucleate and uninucleate spores), the possibility still exists that *V. cheracis* sp. nov. has a disporoblastic sequence resulting in binucleate spores. In other species of *Vairimorpha* and *Nosema*, including the type hosts *V. necatrix* and *N. bombycis*, primary binucleate spores function to disseminate the parasite within the host (Solter and Maddox, 1998).

Before it can be concluded that a disporoblastic sporogony sequence is absent from the life cycle of *V. cheracis* sp. nov., further investigation is required, particularly of yabbies with recently acquired infections in which within-host transmission of the parasite between tissues would be expected to be active. If no disporoblastic sequence is found, it may be explained by the hypothesis that simplification of developmental life cycles reflects recent evolutionary divergences, rather than ancestral patterns (Baker et al., 1997). The dimorphism of *V. necatrix* may be indicative of the ancestral pattern, whereas the loss of either one of the sporogony sequences in more recently evolved species may reflect adaptation by the parasites to the environmental circumstances of the hosts. The abortive nature of the octosporoblastic sequence of *V. imperfecta* may indicate the first stage in the loss of this sequence from the life cycle (Canning et al., 1999).

Pilley (1976) and Mitchell and Cali (1993) found that octosporoblastic sporogony of *V. necatrix* was more frequent at lower ambient temperatures, most notably below 20 °C. Frequency of diplokaryotic spores decreased at lower temperatures. A similar finding was reported for *Vairimorpha mesnili* by Malone and McIvor (1996). In this study, *V. cheracis* sp. nov. infected highland crayfish that for much of the year, live at relatively cool ambient temperatures. It is possible that experiments on the effects of ambient water temperatures on sporogony in *V. cheracis* sp. nov. may reveal the presence of a sporogony sequence resulting in diplokaryotic spores at higher temperatures. Relatively low ambient temperatures and the large size of hosts may account for the slow rate of progress of infection of *V. cheracis* sp. nov. in Australian yabbies, where death occured after several months. In moth larvae infected with *V. imperfecta* or *V. necatrix*, death occured in days to weeks, and the rate of progress of infection was faster at higher temperatures (Canning et al., 1999; Pilley, 1976).

Ultrastructural and developmental features of the octosporoblastic sequence, shared beween the type species *V. necatrix* and *V. cheracis* sp. nov. include the diplokaryotic nature of the sporonts, the separation of the nuclei prior to division of the sporont into two uninucleate daughter cells, the formation of a SPV around the dividing sporont prior to cytokinesis of the sporont daughter cells and the presence of electron dense material in the episporontal space, which appears to be associated with deposition of an electron dense layer on the outside of the rosette-shaped sporogonial plasmodium that develops from the sporont daughter cells. The electron dense inclusions of *V. cheracis* sp. nov. were not as numerous as those in the SPVs of *V. necatrix* (Mitchell and Cali, 1993) or *V. imperfecta* (Canning et al., 1999) and did not form concentric layers as described for these two species. Mitchell and Cali (1993) commented that as *V. necatrix* sporoblasts matured into spores, the amount of electron dense material in the episporontal space of SPVs decreased. This also occurred in the SPVs of *V. cheracis* sp. nov. Canning et al. (1999) observed few fully formed sporoblasts, and no mature spores in the SPVs of *V. imperfecta*, and concluded that the octosporoblastic sequence was abortive. Therefore, comparisons between *V. imperfecta* and *V. cheracis* sp. nov. at the late sporoblast stage of development could not be made. Ultrastructural features of the uninucleate spores shared by *V. cheracis* sp. nov. and *V. necatrix* included the isofilar nature of the polar tube, the lamellar/vesicular nature of the bipartite polaroplast and the dimensions of the outer layer of the polar capsule in relation to the anchoring disc (3:1). Similar numbers of coils of the polar filament occurred in mature octospores; 10–12 in *V. cheracis* sp. nov. and 13–14 in *V. imperfecta*.

The taxonomy of the Microspora is in a period of intense review. Classical methods based on spore morphology and developmental sequences are limited by the relatively small number of useful taxonomic features available, and a paucity of knowledge on the complete life cycles of most species. For example, although research on *T. contejeani* has been conducted for over 100 years, the dimorphic nature of the life cycle of this species has only recently been revealed (Lom et al., 2001). PCR and other molecular technologies for sequencing the DNA of microsporidia are increasingly being used to supplement data gathered by classical methods. Studies based on SSU rDNA sequences have indicated in some cases that classical taxonomic features may not accurately reflect true phylogenetic relationships between species (Weiss and Vossbrinck, 1999). The SSU rRNA gene has been used widely for phylogenetic analyses in the Microspora and other phyla because of the juxtapositon of conserved and nonconserved regions of DNA along its length, facilitating comparisons at various taxonomic levels, including species (McManus and Bowles, 1996). The SSU rRNA gene is the most slowly evolving of the rDNA sequences (Hillis and Dixon, 1991).

In this study, and many others (Baker et al., 1995; Canning et al., 1999, 2002; Malecha, 1983; Muller et al., 2000; Terry et al., 1999), the grouping together of most *Nosema* and *Vairimorpha* species, and the consistent partitioning of the group into two subclades in phylogenetic trees constructed using a variety of methods, suggests that phylogenetic analyses based on SSU

rDNA have validity. With some exceptions, species placed in particular microsporodian genera on the basis of morphological, developmental and ecological features are also grouped together on the basis of similarities in SSU rDNA sequences. The exceptions require more thorough investigation, and may reflect shortcomings in traditional classification systems. Conflicts can only be resolved by careful revision of the taxonomic features used for classification after a more substantial body of molecular and ultrastructural data has been amassed.

Vairimorpha cheracis sp. nov. showed over 97% sequence similarity with *V. imperfecta* and a group of *Nosema* species located in the same subclade. Although the highest sequence similarity was shared with *N. furnacalis* and *N. granulosis*, the presence of an octosporoblastic sporogony sequence precluded placement of *V. cheracis* sp. nov. in the genus *Nosema* because the type description includes only disporoblastic sporogony resulting in binucleate spores (Sprague et al., 1992). SSU rDNA phylogenetic analyses indicated that *V. cheracis* sp. nov. is more distantly related to *V. necatrix* and other members of the subclade in which it occurred, than to members of the subclade that included *V. imperfecta*. It is debatable whether or not the 14% sequence difference between *V. cheracis* sp. nov. and the type species *V. necatrix* is sufficient to place the two species in two different genera. The dilemma of where to draw the line in terms of differentiating genera with respect to DNA sequence similarities or differences has not yet been resolved and it would be premature, at present, to erect a new genus in which to place *V. cheracis* sp. nov.

The intermingling of *Vairimorpha* and *Nosema* species within each of the two subclades illustrated in Fig. 17 suggests that separation of these two genera on the basis of developmental life cycle characteristics may not accurately represent their true relationships. Also, in the light of the molecular phylogenetic analyses, allocation of *Vairimorpha* species and *Nosema* species to different families (Burenellidae and Nosematidae, respectively) according to Sprague et al. (1992), seems nonsensical. Canning et al. (1999) suggested that it would be more appropriate to classify all *Vairimorpha* and *Nosema* species in one family, Nosematidae, until a taxonomic review can be conducted. The fire ant pathogen, *V.* sp. FA was placed at a sufficient distance from the *Vairimorphal Nosema* clade to suggest it should not be included in the genus *Vairimorpha* or in the same family, and should be reclassified. Moser et al. (1998) also remarked that reclassification of *Vairimorpha* sp. FA is warranted. It is possible that the microsporidian parasite of New Zealand crayfish, *Paranephrops zealandicus*, identified by Quilter (1976) as *Thelohania contejeani* (Henneguy and Thelohan, 1892), was in fact a species of *Vairimorpha*, based on spore shape and size, SPV membrane persistence, and the fact that only octosporous vesicles with uninucleate spores were reported. The collection of additional ultrastructural, molecular and life cycle data on *Nosema* and *Vairimorpha*-like microsporidia from crustacean and insect hosts would enable a detailed taxonomic review to be carried out. Hopefully the issues discussed above would be resolved in the process.

Most spores and earlier developmental stages of *V. cheracis* sp. nov. were found in crayfish muscle tissue. Uninucleate spores in octosporous vesicles are most likely to have been formed by meiosis (Canning, 1988; Flegel and Pasharawipas, 1995), and in *V. cheracis* sp. nov., they are presumably formed for horizontal transmission to the next host. The relatively persistent vesicles may help to maintain the viability and infectivity of spores after death of the host yabby, and during transit through the digestive system of the next host. It is possible that an intermediate host is involved in horizontal transmission of *V. cheracis* sp. nov. Studies on microsporidia parasitic in mosquito hosts have revealed that in several genera, including *Amblyospora*, *Duboscquia*, *Hyalinocysta*, and *Parathelohania*, a copepod intermediate host is involved in transmission of uninucleate spores to the next mosquito host (Andreadis, 1990, 1999; Andreadis and Vossbrinck, 2002; Becnel, 1994; Sweeney and Graham, 1988; Sweeney et al., 1985, 1989, 1993). The inclusion of an intermediate host in the life cycle may help to ensure survival of microsporidia in aquatic environments subject to the vagaries of drought and flood. Indirect horizontal transmission is facilitated in such environments by overlapping generations of definitive and intermediate aquatic hosts (Andreadis and Vossbrinck, 2002).

The presence of spores within the intestinal wall of infected yabbies indicates a possible oral route of infection, although the spores seen in Fig. 15 were contained in SPVs. This is unusual with respect to within-host transmission, usually effected by free binucleate spores in other species of dimorphic microsporidians (Becnel and Andreadis, 1999). The majority of other *Vairimorpha* and *Nosema* species infect gut epithelium, fat body cells, glandular cells, and gonadal tissues of their arthropod hosts (Canning et al., 1999; Mitchell and Cali, 1993; Pilarska et al., 2002; Pilley, 1976; Terry et al., 1999).

The potential for vertical transmission of *V. cheracis* sp. nov. was suggested by the discovery of spores immediately outside the follicular cells in the ovary of a female yabby. Again, however, the spores were in SPVs, i.e., not the typical diplokaryotic free spores responsible for transovarial transmission in other *Vairimorpha* or *Nosema* species (Becnel and Andreadis, 1999). Direct horizontal transmission between hosts by the oral route and vertical transmission from mother to progeny via

eggs, have been described for other species of *Vairimorpha* including *V. imperfecta* and *V. necatrix*, and for many *Nosema* species which infect insects (Becnel and Andreadis, 1999; Canning et al., 1999; Pilley, 1976). The amphipod parasite, *N. granulosis*, is only transmitted vertically, which may explain the absence of uninucleate octospores in its life cycle. Conversely, the dominance of uninucleate octospores in the life cycle of *V. cheracis* sp. nov. suggests horizontal transmission is most important in this species. Transmission pathways in the lifecycle of *V. cheracis* sp. nov. require further investigation.

The microsporidian parasites of Australian aquatic invertebrates other than mosquitoes are a poorly known group. Many of the reports in the literature are of undescribed species and very little is known about their biology (O'Donoghue and Adlard, 2000). This is the first record of a *Vairimorpha* species which is a parasite of a crustacean host. *V. cheracis* sp. nov. can be differentiated from other microsporidians by examining the morphological and ultrastructural features described in Table 4, or more readily, by using molecular tools such as polymerase chain reaction (PCR) assays based on the SSU rDNA sequence presented above. The Australian yabby, *C. destructor*, is a species of economic importance in freshwater aquaculture, and as such, further research on the geographic ranges, host ranges, life cycles, transmission routes, and general ecology of microsporidian parasites such as *V. cheracis* sp. nov. will be extremely valuable to disease control and prevention programs associated with intensive aquaculture of the host species. Further sequencing of key genes of microsporidian parasites will allow more accurate taxonomic revisions to be carried out on members of this enigmatic phylum, facilitate biogeographical studies and contribute to our understanding of microsporidian evolution.

***Taxonomic summary—Vairimorpha cheracis* sp. nov.**

Type host. The freshwater crayfish, *Cherax destructor* (Clark)

Transmission. Unknown

Site of infection. Muscle tissue of male and female hosts, intestinal mucosa, intercellular spaces between follicular cells surrounding the ova.

Interface. Very early sporonts in direct contact with host cell cytoplasm. Octosporous sporulation within sporophorous vesicle, produced by the sporont.

Other parasite–host relations. Muscle cells become packed with parasites.

Haplophase. Only uninucleate spores observed. The majority in ovoid sporophorous vesicles.

Merogony. Not observed.

Transition to sporogony. Ovoid diplokaryotic sporont with a thickened plasmalemma.

Sporogony. Only octosporoblastic sporogony observed. Sporont divides into two uninucleate daughter cells within the sporophorous vesicle. Each daughter cell divides into four uninucleate sporoblasts. Cytokinesis not completed until after rosette-shaped plasmodium is formed. Plasmodium divides and eight uninucleate sporoblasts mature within sporophorous vesicle.

Spore. Only pyriform uninucleate spores observed. Dimensions: $3.4 \times 1.9\,\mu m$ (range $3.0–3.8 \times 1.7–2.3\,\mu m$), $n = 40$. Lateral exospore: 31 nm in width, lateral endospore: 52 nm in width ($n = 10$). Isofilar polar filament with 10–12 coils. Anterior polaroplast lamellar, posterior polaroplast vesicular. Moderate to large posterior vacuole.

Type locality. Tea Tree Creek (30°30′S, 151°29′E), 20 km west of Armidale, NSW, Australia.

Remarks. Only heavily infected adult yabbies were sampled. Phylogenetic studies based on SSU rDNA indicate that *V. cheracis* sp. nov. is closely related to *V. imperfecta*, and a group of *Nosema* species including *N. granulosis* and *N. furnacalis*. In phylogenetic trees constructed using distance criteria, maximum parsimony criteria and Bayesian inference, the *Nosema*/*Vairimorpha* group of species was divided into two subclades. *V. cheracis* sp. nov. was placed in a different subclade to that containing the type species, *V. necatrix*. Type specimens were deposited in the Queensland Museum, Brisbane, Australia. Registration number for hapantotype: G463720; parahapantotype: G463721. The nucleotide sequence of *V. cheracis* sp. nov. SSU rDNA was deposited in GenBank under Accession No. AF327408.

Acknowledgments

This research was supported by a joint scholarship from the University of New England and CSIRO, Livestock Industries. The authors particularly thank the following people for their assistance: Dr. Robert Adlard, Dr. Carlos Azevedo, Dr. Jeremy Bruhl, Professor Iva Dykova, Mr. Zoltan Enoch, Mr. Peter Garlick, Professor Robin Gasser, Dr. Dean Jerry, Ms. Mahri Koch, Mr. Ian Lenane, Mr. Callum Mack, Dr. Jennifer Mathews, Dr. Mary Notestine, Dr. Peter O'Donoghue, Professor Klaus Rohde, Dr. Jessica Worthington-Wilmer, and Dr. Tony Sweeney.

References

Andreadis, T.G., 1990. Epizootology of *Amblyospora connecticus* (Microsporida) in field populations of the saltmarsh mosquito, *Aedes cantator*, and the cyclopoid copepod, *Acanthocyclops vernalis*. J. Protozool. 37, 174–182.

Andreadis, T.G., 1999. Epizootology of *Amblyospora stimuli* (Microsporidiida: Amblyosporidae) infections in field populations of a univoltine mosquito, *Aedes stimulans* (Diptera: Culicidae), inhabiting a temporary vernal pool. J. Invertebr. Pathol. 74, 198–205.

Andreadis, T.G., Vossbrinck, C.R., 2002. Life cycle, ultrastructure and molecular phylogeny of *Hyalinocysta chapmani* (Microsporidia: Thelohaniidae), a parasite of *Culiseta melanura* (Diptera: Culicidae)

and *Orthocyclops modestus* (Copepoda: Cyclopidae). J. Eukaryot. Microbiol. 49, 350–364.

Austin, C.M., 1996. Systematics of the freshwater crayfish genus *Cherax* Erichson (Decapoda: Parastacidae) in northern and eastern Australia: electrophoretic and morphological variation. Aust. J. Zool. 44, 259–296.

Baker, M.D., Vossbrinck, C.R., Becnel, J.J., Maddox, J.V., 1997. Phylogenetic position of *Amblyospora* Hazard and Oldacre (Microspora: Amblyosporidae) based on small subunit rRNA data and its implication for the evolution of Microsporidia. J. Eukaryot. Microbiol. 44, 220–225.

Baker, M.D., Vossbrinck, C.R., Didier, E.S., Maddox, J.V., Shadduck, J., 1995. Small subunit ribosomal DNA phylogeny of various microsporidia with emphasis on AIDS related forms. J. Eukaryot. Microbiol. 42, 564–570.

Becnel, J.J., 1994. Life cycles and host–parasite relationships of microsporidia in culicine mosquitoes. Folia Parasitol. 41, 91–96.

Becnel, J.J., Andreadis, T.G., 1999. Microsporidia in insects. In: Wittner, M., Weiss, L.M. (Eds.), The Microsporidia and Microsporidiosis. ASM Press, Washington DC, pp. 447–501.

Briano, J.A., Williams, D.F., 2002. Natural occurrence and laboratory studies of the fire ant pathogen *Vairimorpha invictae* (Microsporida: Burenellidae) in Argentina. Environ. Entomol. 31, 887–894.

Cali, A., Takvorian, P.M., Lewin, S., Rendel, M., Sian, C.S., Wittner, M., Tanowitz, H.B., Keohane, E., Weiss, L.M., 1998. *Brachiola vesicularum*, n. g., n. sp., a new microsporidium associated with AIDS and myositis. J. Eukaryot. Microbiol. 45, 240–251.

Canning, E.U., 1988. Nuclear division and chromosome cycle in microsporidia. Biosystems 21, 333–340.

Canning, E.U., Curry, A., Cheney, S., Lafranchi-Tristem, N.J., Haque, M.A., 1999. *Vairimorpha imperfecta* n.sp., a microsporidian exhibiting an abortive octosporous sporogony in *Plutella xylostella* L. (Lepidoptera: Yponomeutidae). Parasitology 119, 273–286.

Canning, E.U., Refardt, D., Vossbrinck, C.R., Okamura, B., Curry, A., 2002. New diplokaryotic microsporidia (Phylum Microsporidia) from freshwater bryozoans (Bryozoa, Phylactolaemata). Europ. J. Protistol. 38, 247–265.

Flegel, T.W., Pasharawipas, T., 1995. A proposal for typical eukaryotic meiosis in microsporidians. Can. J. Microbiol. 41, 1–11.

Fowler, J.L., Reeves, E.L., 1974. Spore dimorphism in a microsporidian isolate. J. Protozool. 21, 538–542.

Henneguy, G., Thelohan, P., 1892. Myxosporides parasites des muscles chez quelques crustaces decapodes. Ann. Microgr. 4, 617–641.

Hillis, D.M., Dixon, M.T., 1991. Ribosomal DNA: molecular evolution and phylogenetic inference. Quart. Rev. Biol. 66, 411–453.

Huelsenbeck, J.P., Ronquist, F., 2001. MRBAYES: Bayesian inference of phylogenetic trees. Bioinformatics 17, 754–755.

Jeanmougin, F., Thompson, J.D., Gouy, M., Higgins, D.G., Gibson, T.J., 1998. Multiple sequence alignment with Clustal X. Trends Biochem. Sci. 23, 403–405.

Jouvenaz, D.P., Hazard, E.I., 1978. New family, genus and species of microsporida (Protozoa: Microsporida) from the tropical fire ant, *Solenopsis geminata* (Fabricius) (Insecta: Formicidae). J. Protozool. 25, 24–29.

Kramer, J.P., 1965. *Nosema necatrix* sp. n. and *Thelohania diazoma* sp.n. from the armyworm *Pseudaletia unipunctata* (Haworth). J. Invertebr. Pathol. 7, 117–121.

Labbe, A., 1899. Sporozoa. In: Butschi, O. (Ed.), Das Tierrich. Friedlander u Sohn, Berlin.

Langdon, J.S., 1991. Description of *Vavraia parastacida* sp. nov. (Microspora: Pleistophoridae) from marron, *Cherax tenuimanus* (Smith), (Decapoda: Parastacidae). J. Fish. Dis. 14, 619–629.

Lom, J., Nilsen, F., Dykova, I., 2001. *Thelohania contejeani* Henneguy, 1892: dimorphic life cycle and taxonomic affinities, as indicated by ultrastructural and molecular study. Parasitol. Res. 87, 860–872.

Malecha, S.R., 1983. Crustacean genetics and breeding: an overview. Aquaculture 33, 395–413.

Malone, L.A., McIvor, C.A., 1996. Use of nucleotide sequence data to identify a microsporidian pathogen of *Pieris rapae* (Lepidoptera, Pieridae). J. Invertebr. Pathol. 68, 231–238.

McManus, D.P., Bowles, J., 1996. Molecular genetic approaches to parasite identification: their value in diagnostic parasitology and systematics. Int. J. Parasitol. 26, 687–704.

Mitchell, M.J., Cali, A., 1993. Ultrastructural study of the development of *Vairimorpha necatrix* (Kramer, 1965) (Protozoa, Microsporida) in larvae of the corn earworm, *Heliothis zea* (Boddie) (Lepidoptera, Noctuidae) with emphasis on sporogony. J. Eukaryot. Microbiol. 40, 701–710.

Moodie, E.G., Le Jambre, L.F., Katz, M.E., 2003a. *Thelohania parastaci* sp. nov. (Microspora: Thelohaniidae), a parasite of the Australian freshwater crayfish, *Cherax destructor* (Decapoda: Parastacidae). Parasitol. Res. 91, 151–165.

Moodie, E.G., Le Jambre, L.F., Katz, M.E., 2003b. *Thelohania montirivulorum* sp. nov. (Microspora:Thelohaniidae), a parasite of the Australian freshwater crayfish, *Cherax destructor* (Decapoda: Parastacidae): fine ultrastructure, molecular characteristics, and phylogenetic relationships. Parasitol. Res. 91, 215–228.

Moser, B.A., Becnel, J.J., Maruniak, J., Patterson, R.S., 1998. Analysis of the ribosomal DNA sequences of the microsporidia *Thelohania* and *Vairimorpha* of Fire Ants. J. Invertebr. Pathol. 72, 154–159.

Muller, A., Trammer, T., Chioralia, G., Seitz, H.M., Diehl, V., Franzen, C., 2000. Ribosomal RNA of *Nosema algerae* and phylogenetic relationship to other microsporidia. Parasitol. Res. 86, 18–23.

Naegeli, C., 1857. Uber die neue Krankheit der Seideraupe und verwandte Organismen. Bot. Ztg. 15, 760–761.

O'Donoghue, P., Beveridge, I., Phillips, P., 1990. Parasites and ectocommensals of yabbies and marron in South Australia. Report to the South Australian Department of Agriculture, Central Veterinary Laboratories (VETLAB).

O'Donoghue, P.J., Adlard, R.D., 2000. Catalogue of Protozoan Parasites Recorded in Australia. Memoirs of the Queensland Museum 45, 1–163.

Pilarska, D., Linde, A., Solter, L.F., Takov, D., McManus, D.P., Goertz, D., 2002. Ultrastructure characteristic of a *Nosema* sp. (Microsporidia) from a Bulgarian population of *Euproctis chrysorrhoea* L. (Lepidoptera). Acta Parasitol. 47, 1–5.

Pilley, B.M., 1976. A new genus, *Vairimorpha* (Protozoa: Microsporida), for *Nosema necatrix* Kramer 1965: pathogenicity and life cycle in *Spodoptera exempta* (Lepidoptera: Noctuidae). J. Invertebr. Pathol. 28, 177–183.

Posada, D., Crandall, K.A., 1998. MODELTEST: testing the model of DNA substitution. Bioinformatics 14, 817–818.

Quilter, C.G., 1976. Microsporidian parasite *Thelohania contejeani* Henneguy from New Zealand freshwater crayfish. NZ. J. Mar. Freshw. Res. 10, 225–231.

Rice, R.N., 2001. Nosema disease in honeybees—genetic variation and control. Report to Rural Industries Research and Development Corporation, Publication No. 01/46, 36 pages. ACT, Australia: Rural Industries Research and Development Corporation.

Solter, L.F., Maddox, J.V., 1998. Timing of an early sporulation sequence of microsporidia in the genus *Vairimorpha* (Microsporidia: Burenellidae). J. Invertebr. Pathol. 72, 323–329.

Sprague, V., 1950. *Thelohania cambari* n. sp., a microsporidian parasite of North American crayfish. J. Parasitol. (Suppl) 36, 46.

Sprague, V., 1966. Two new species of *Plistophora* (Microsporida, Nosematidae) in decapods with particular reference to one in the blue crab. J. Protozool. 13, 196–199.

Sprague, V., Becnel, J.J., Hazard, E.J., 1992. Taxonomy of Phylum Microspora. Crit. Rev. Microbiol. 18, 285–395.

Sweeney, A.W., Graham, M.F., 1988. Life cycle of *Amblyospora dyxenoides* sp. nov. in the mosquito *Culex annulirostris* and the copepod *Mesocyclops albicans*. J. Invertebr. Pathol. 51, 46–57.

Sweeney, A.W., Hazard, E.I., Graham, M.F., 1985. Intermediate host for an *Amyblyospora* sp. (Microspora) infecting the mosquito, *Culex annulirostris*. J. Invertebr. Pathol. 46, 98–102.

Sweeney, A.W., Doggett, S.L., Gollick, G., 1989. Bioassay experiments on the dose response of *Mesocyclops* sp. copepods to meiospores of *Amblyospora dyxenoides* produced in *Culex annulirostris* mosquito larvae. J. Invertebr. Pathol. 53, 118–120.

Sweeney, A.W., Doggett, S.L., Piper, R.G., 1993. Life cycle of a new species of *Duboscquia* (Microsporida: Thelohaniidae) infecting the mosquito *Anopheles hilli* and an intermediate copepod host, *Apocyclops dengizicus*. J. Invertebr. Pathol. 62, 137–146.

Swofford, D.L., 2000. PAUP*. Phylogenetic analysis using parsimony (*and other methods), version 4. Sinauer Associates, Sunderland, USA.

Terry, R.S., Smith, J.E., Bouchon, D., Rigaud, T., Duncanson, P., Sharpe, R.G., Dunn, A.M., 1999. Ultrastructural characterisation and molecular taxonomic identification of *Nosema granulosis* n. sp., a transovarially transmitted feminising (TTF) microsporidium. J. Eukaryot. Microbiol. 46, 492–499.

Undeen, A., 1997. Microsporidia (Protozoa): A Handbook of Biology and Research Techniques. Available from http://pearl.agcomm.okstate.edu:16080/scsb387/content.htm Accessed 6 December 2003. Gainesville, Florida, USA: Center for Medical, Agricultural and Veterinary Entemology.

Unestam, T., 1973. Significance of diseases on freshwater crayfish. Freshwater Crayfish 1, 135–150.

Vavra, J., Undeen, A.H., 1970. *Nosema algerae* n. sp. (Cnidospora, Microsporida), a pathogen in a laboratory colony of *Anopheles stephensi* Liston (Diptera, Culicidae). J. Protozool. 17, 240–249.

Weiss, L.M., Vossbrinck, C.R., 1998. Microsporidiosis: Molecular and Diagnostic Aspects. In: Tzipori, S. (Ed.), Opportunistic Protozoa in Humans. Academic Press, London, pp. 351–395.

Weiss, L.M., Vossbrinck, C.R., 1999. Molecular Biology, Molecular Phylogeny, and Molecular Diagnostic Approaches to the Microsporidia. In: Wittner, M., Weiss, L.M. (Eds.), The Microsporidia and Microsporidiosis. ASM Press, Washington DC, pp. 129–171.